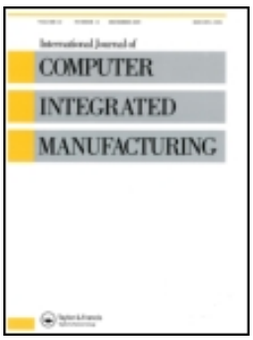

International Journal of Computer Integrated Manufacturing

ISSN: 0951-192X (Print) 1362-3052 (Online) Journal homepage: http://www.tandfonline.com/loi/tcim20

Task-oriented configuration design for reconfigurable parallel manipulator systems

A. K. Dash , I. -M. Chen , S. H. Yeo & G. Yang

To cite this article: A. K. Dash , I. -M. Chen , S. H. Yeo & G. Yang (2005) Task-oriented configuration design for reconfigurable parallel manipulator systems, International Journal of Computer Integrated Manufacturing, 18:7, 615-634, DOI: 10.1080/09511920500069192

To link to this article: http://dx.doi.org/10.1080/09511920500069192

International Journal of Computer Integrated Manufacturing, Vol. 18, No. 7, October – November 2005, 615 – 634

Task-oriented configuration design for reconfigurable parallel manipulator systems

A. K. DASH*†, I.-M. CHEN†, S. H. YEO† and G. YANG‡

†School of Mechanical and Production Engineering Nanyang Technological University, Nanyang Avenue, Singapore-639798
‡Mechatronics Division, Singapore Institute of Manufacturing Technology, Singapore-638075

A reconfigurable parallel manipulator system consists of an inventory of standard interchangeable actuator modules, passive joint modules and customizable links and connectors. Owing to the interchangeability and modularity, a parallel manipulator constructed in this manner can have different structures and degrees of freedom (DOF). This article presents a two-stage design methodology, from structure determination to parameter optimization, for determining task-specific optimal configurations of reconfigurable parallel manipulators. In the structure determination stage, a reconfigurable robot assembly database containing the possible parallel manipulator assemblies is established based on enumeration. A TaskToRobot Map is proposed to map the given task description to a suitable manipulator configuration in the database according to the DOFs of the required task. In the parameter optimization stage, design parameters of the selected manipulator structure, such as link lengths, dimensions of the connectors and actuation schemes are identified. As these parameters contain continuous and discrete variables, synthesis of the manipulator parameters is formulated based on a Simplex optimization method. This design methodology is demonstrated effectively in the selection of a reconfigurable parallel manipulator system for a light machining operation.

Keywords: Parallel manipulation; Reconfigurable robots; Task-oriented design; Optimal design

1. Introduction

Next-generation manufacturing will involve application of new concepts, models, methodologies and information technologies, with the goal of preparing manufacturing companies to become more competitive in a global and networked environment. In this regard, the growing use of parallel manipulators in manufacturing industries indicates that it is a suitable machine for the future. Applications of parallel manipulators are commonly found in the motion platform for pilot training simulators, positioning devices for high-precision surgical tools, parallel-type multi-axis machining tools and precision assembly tools. A parallel manipulator is a closed-loop mechanism in which the mobile platform is connected to the base by at least two serial kinematic chains (legs). It has high structural rigidity, high positioning capability, high accuracy and high strength-to-weight ratio. However, the design, trajectory planning and application developments of parallel robots are challenging owing to the closed-loop nature of the mechanism. The modular concept has emerged to address such issues (Yang *et al*., 2001, Cohen *et al*., 1992). To date, several prototype modular robotics systems have been demonstrated in various research institutes, such as the Carnegie Melbon University (CMU) reconfigurable modular manipulator system (RMMS), modular robotics system at Toronto, Toshiba Modular Manipulator System (TOMMS) at the Toshiba Corporation, etc. Basically, these systems have serial-type geometry with large working envelopes. Using fixed- and variable-dimension modules, the modular robotics group at Nanyang Technological University and Singapore Institute of Manufacturing

*Corresponding author. Email: michen@ntu.edu.sg

International Journal of Computer Integrated Manufacturing
ISSN 0951-192X print/ISSN 1362-3052 online © 2005 Taylor & Francis
http://www.tandf.co.uk/journals
DOI: 10.1080/09511920500069192

Technology have developed serial, parallel and hybrid-type modular robotic workcells. A reconfigurable parallel robot consists of a set of independently designed modules, such as actuators, passive joints, rigid links (connectors), mobile platforms and end-effectors that can be rapidly assembled into various configurations with different kinematic characteristics and dynamic behaviours. Therefore, developing a methodology for the reconfigurable robot system to determine a robot configuration for a specific task is an important issue.

For serial-type reconfigurable robots, Ambrose (1991) presented a methodology for matching tasks to reconfigurable robots. An initial set of joint and link modules is tested for selected performance requirements. Then module combinations are matched with user-specified task requirements to search for the best solution. Paredis (1996) has used an agent-based approach to solve the task-based design of CMU's reconfigurable manipulator system. Kim and Khosla (1993) addressed the task-based design of manipulators for space shuttle tile servicing. The dexterity measure is taken as the ultimate criterion and the task/manipulator specification as the design constraints. A multi-population Genetic Algorithm (GA) executed in parallel is used for optimization. Chen (1994) formulates the task-oriented optimal configuration problem as a combinatorial optimization problem. The formulation is based on an assembly incidence matrix (AIM) representation of a reconfigurable robot. The task requirement is defined as a set of sequential working points (positions) in the task space. Yang (1999) has used a minimal degrees of freedom (DOF) concept to find the robot with the least DOFs as the optimal solution for a given task.

Tsai (2000) introduced a design methodology for parallel mechanisms based on graph theory and combinatorial analysis. Podhorodeski and Pittens (1994) studied the enumeration scheme of parallel manipulators consisting of serial branches acting in parallel on a common end-effector. Similar to these results were the results of Yang *et al*. (2001). They presented a type synthesis of a class of three-legged reconfigurable in-parallel robots using two types of sub-assemblies, namely standard, fixed-dimension modules and variable-dimension modules. Considering leg interference and symmetry, a three-legged robot geometry is chosen as the norm of reconfigurable parallel robot design. Merlet (2000) has presented an exhaustive enumeration of mechanical architectures of parallel robots. The list is classified by increasing number of DOFs, from two to six, for the end-effector. Merlet also presented a design methodology (Merlet 1997) for Gough-type parallel robots to satisfy a set of performance constraints. Park (1995) used differential geometry in formulating meaningful performance measures for parallel manipulators that are independent of the choice of coordinate frames. A global coordinate-free method of differential geometry is used in formulating the global kinematic and dynamic properties. In addition to the above works, there are many other contributions in the design of parallel manipulators (Stamper *et al.,* 1997, Kim and Ryu 2001 and Ryu and Cha 2001).

The challenge in reconfigurable parallel manipulator design is the task of finding a suitable topology of a parallel manipulator for a specific task automatically. Once a topology is selected, the design variables affect its performance (singularity, manipulability, stiffness and accuracy, etc.) in a complicated manner. The design variables considered here are geometry of the mechanism and the actuation scheme. Among these, the effect of the actuation scheme of the active joints on the optimal design of parallel manipulators has not been studied extensively in the literature. The actuation scheme is the sequence in which the joints of a leg are actuated.

In this paper, the design of reconfigurable parallel robots is divided into two stages: the structure determination stage and the parameter determination stage. The necessity of intervention of the designer in the structure determination stage divides the whole process into two stages. In the structure determination stage, to select an appropriate parallel manipulator, a reconfigurable robot assembly database is created by enumeration of fixed and variable dimension modules. This database contains various topologies of parallel manipulators having different DOF. Then, a specific topology is selected by using `TaskToRobot` map for the task at hand. `TaskToRobot` map, which is built on the knowledge of the designer, is a table which maps different tasks to suitable reconfigurable parallel manipulators in the database. The mapping of the tasks depends upon the DOF involved in the task specifications. By this, automatic selection of configurations, which preempts the designer's knowledge, is avoided. Subsequently, in the parameter determination stage, design variables are identified that include the actuation scheme along with the link parameters of a parallel manipulator. A detailed study on the effect of the actuation scheme on performance of reconfigurable parallel manipulators is discussed. A nonlinear constraint single-objective design optimization problem is formulated and solved to determine the optimal values of these design parameters. A Simplex optimization toolbox of Matlab is used for implementation.

The rest of this paper is organized as follows: section 2 outlines the task description; section 3 describes the structure-determination stage; section 4 describes parameter-determination stage; a case study is discussed in section 5 and section 6 concludes the paper.

2. Task description

A typical task description includes information leading to structure determination and parameter determination

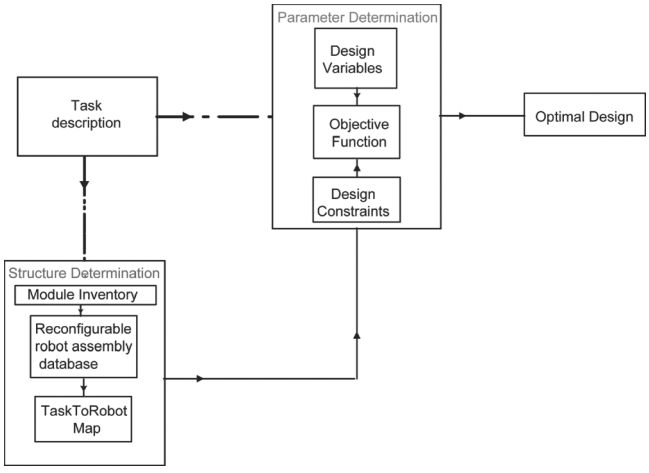

Figure 1. The flow of the task-optimal design algorithm.

(figure 1). As shown in figure 1, task description in a task-based design plays an important role in the structure and parameter determination of parallel manipulators.

Information that leads to structure determination includes, for example, the need for a reconfigurable machine in an assembly line, capability of performing three-DOF planar and six-DOF spatial motions, etc. This kind of information is translated into functional requirements (see section 3.2.1) and subsequently to the structural characteristics of the machine. They also play an important role in selecting suitable topologies of machines determined from `TaskToRobot` map.

Information leading to parameter determination includes various performance indices such as accuracy, stiffness, reachability, manipulability, etc. It also includes maximum power consumption, floor space availability, joint range limitation (in case of an existing module inventory), etc. This information helps in formulating design constraints or the objective function of the optimization problem.

3. Structure determination stage

In the case of parallel manipulators, the process of a suitable topology for a specific task is very important and difficult. Completely automatizing it may not give the best result. This process requires designer's knowledge. In this article, a suitable parallel manipulator topology is selected with the help of a `TaskToRobot` map. Following this, the designer chooses the best topology out of the selected topologies. Thus the complete design process is broken down to two stages: the structure determination stage and the parameter determination stage. The structure determination stage is shown in figure 1. In this stage, a reconfigurable robot assembly database is created using the inventory of modules. Based on this, the `TaskToRobot` map is created, which maps the task to suitable parallel topologies.

3.1. *Module inventory*

Different components of a reconfigurable parallel manipulator include actuators, the end-effector, connecting linkages, the mobile platform, the passive three-DOF spherical joints, passive two-DOF universal joints, one-DOF passive joints, etc. The closed-loop nature of parallel mechanisms imposes kinematic constraints on the dimensions of robot sub-assemblies and makes the construction of a useful parallel manipulator challenging from entirely standard modules. To overcome this, two types of sub-assemblies are used to modularize a parallel robot: fixed-dimension modules and variable dimension modules (Yang *et al.*, 2001).

3.1.1. Fixed-dimension modules. The fixed-dimension modules include actuator modules, passive joint modules and end-effector modules. For the sake of reconfigurability, the actuator modules and the end-effector modules must be compact, self-contained and intelligent mechatronic drive units. Figure 2(a) is a prismatic and figure 2(b) is a revolute actuator module. In the module inventory, there are two varieties of these actuators to accommodate different payloads. The connection between modules is through mechanical means.

Three types of passive joint modules (without actuators) are in-house designed and fabricated. Figures 3(a)–(c) are respectively a pivot joint, a rotary joint and a spherical joint. The pivot joint [as shown in figure 3(a)] and the rotary joint [as shown in figure 3(b)] provide a rotational DOF about an axis normal to the link axis and a rotational DOF about the axis of the link, respectively. Angular displacement sensors are built into the passive rotary and pivot joint modules for forwards displacement sensing of the parallel manipulators.

3.1.2. Variable-dimension modules. Rigid links, module connectors, and mobile platforms are the modules that can be designed with customized dimensions. By allowing dimensional change in module design, the end-user is given the ability to rapidly fine-tune the kinematic and dynamic performance of the completed manipulator. A set of links with various geometrical shapes and dimensions [figure 4(a)] and a mobile platform [figure 4(b)] have been designed and fabricated.

3.2. *Reconfiguration*

To achieve reconfiguration, a very simple manual connection method is used in the module hardware design. It is based on the flange-type rigid connectors/links [figure 4(a)]. The flanges tightly connect the active and passive joint

modules through bolts and nuts. Stepping links and angle plates are also designed with flanges. Although it lacks quick connection capability, it allows different types of modules to be connected together easily. Figure 5 shows a fleet of modular robots made out of these modules, designed and constructed in the current authors' laboratory.

3.3. *Reconfigurable robot assembly database*

The reconfigurable robot assembly database is the result of enumeration of various topologies of reconfigurable parallel manipulators using the inventory of modules. Enumeration of the configurations of parallel manipulators is performed according to their nature of motion and DOF. Guidelines are required to enumerate these mechanisms and these guidelines come from the customer's needs such as DOF, workspace, stiffness, accuracy, etc. As mentioned by Ullman (1992), the design process is divided into three inter-related phases:

1. product specification and planning phase;
2. conceptual design phase;
3. product design phase.

During the product specification and planning phase, some of the customer's needs are identified and translated into engineering specifications in terms of functional requirements, time and cost available for the development, and the project is planned accordingly. Some of these functional requirements are utilized for enumeration of the mechanisms.

3.3.1. Functional requirements. In this work, enumeration of kinematic structures of parallel manipulators is of interest, using the types of modules available in the inventory. The functional requirements of a reconfigurable

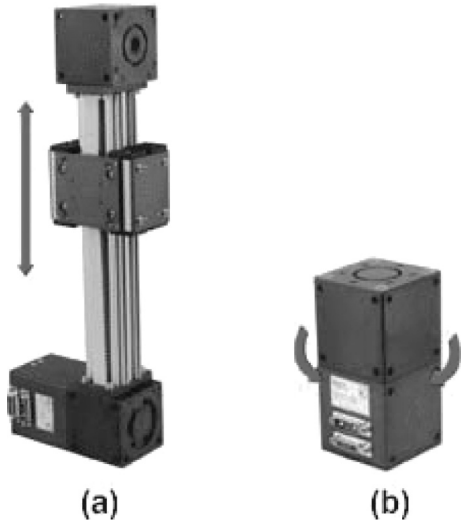

Figure 2. (a) Prismatic actuator module; (b) revolute actuator module.

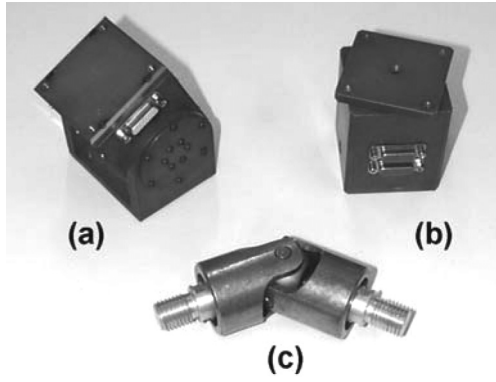

Figure 3. Passive joint modules: (a) pivot joint; (b) rotary joint; (c) spherical joint.

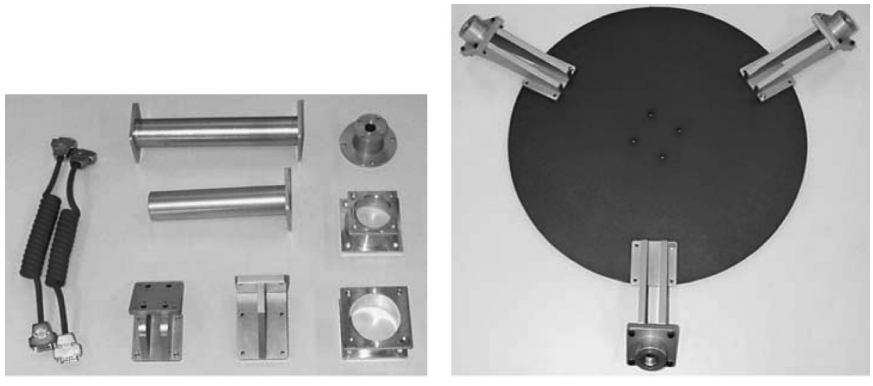

(a) (b)

Figure 4. Links, connector modules and mobile platform.

Figure 5. Reconfigurable manipulators.

parallel manipulator system are hypothetically stated as follows.

1. As the focus of this study is on parallel manipulators, only closed-loop mechanisms are considered. Specifically they consist of a moving platform connected to a fixed base by more than one limb. The end-effector is mounted on the moving platform.
2. Depending upon the specific task to be performed, there are multiple DOF of the end-effector.
3. The manipulator has nonredundant actuation (to simplify the design process and the control scheme) and the number of legs is equal to or less than the number of DOF (so that each leg has at least one actuator). Preferably, the actuators are arranged symmetrically among the limbs. Fewer number of legs are preferred because of less chance of interference.
4. Leg symmetry is an advantage for parallel manipulators when uniform force distributions among the supporting legs and robot configuration control are considered. Thus manipulator configurations limited to two, three and six legs are enumerated. For the same reason, the design process is simplified to two-, three- and six-DOF motions because leg symmetry is not obtained for any other DOF motion.
5. Because of their weight, the total number of active and passive joint modules is kept at a minimum. The prismatic module under consideration is much heavier and bulkier than the revolute joint module. The prismatic joint included in a chain should be mounted close to the base. In the design here, the prismatic joint will only be considered at the first or second joint from the base. Owing to space constraint and the possibility of leg interference, only one prismatic joint is used per leg.
6. Since the actuator modules are cubic in shape, successive joint directions are parallel or perpendicular to each other.
7. Spherical joint modules with three-DOFs are preferable for the legs of the robots in reducing the number of passive-joint modules. There are only four types of passive joints belonging to the rotary type: the one-DOF revolute joint, the one-DOF pivot joint, the two-DOF universal joint and the three-DOF spherical joint.

3.3.2. Structural characteristics. In this section, functional requirements are converted into structural characteristics so that these structural characteristics are incorporated as rules to enumerate all possible solutions of parallel manipulators via combinatorial analysis (Tsai 2000). Except for some overconstrained mechanisms, the DOF of a mechanism is governed by

$$d = \lambda(n - j - 1) + \sum_i d_i \tag{1}$$

where λ is the dimension of the workspace in which a mechanism is intended to function (for example for planar and spatial mechanisms λ is 3 and 5, respectively), d is the DOF of a mechanism, n is the number of links in a mechanism and j is the number of joints in a mechanism. All joints are binary, and d_i DOF is associated with joint i.

The relationship between the number of independent loops, l, the number of joints, j, and the number of links, n, in a mechanism is given by Euler's equation

$$l = j - n + 1 \tag{2}$$

Eliminating n and j from equations (1) and (2), yields the loop-mobility criterion as

$$\sum d_i = d + \lambda l \tag{3}$$

It is assumed that each limb in a parallel manipulator is made up of a simple open-loop chain. As mentioned in section 3.2.1, the design process is simplified to two, three and six legs in two-, three- and six-DOF motions. Among these, in the category of six-DOF motion mechanisms, there can be three or six legs to ensure leg symmetry (refer to tables 1 and 2). In the rest two cases namely two and three-DOF motions, there will be as many numbers of legs as there are degrees of freedoms. Thus, it can be shown for all manipulators except the six-DOF manipulators that

$$m = d = l + 1 \tag{4}$$

where m is the number of limbs in a parallel manipulator.

Table 1. Enumeration of actuation scheme of six-DOF non-redundant parallel manipulator [adapted from Podhorodeski and Pittens (1994)].

Number of legs in-parallel	Number of actuated single degree-of-freedom joints in each leg
2	3,3
3	3,3,0
	1,1,4
	1,2,3
	2,2,2
6	1,1,1,1,1,1

Table 2. Classification of spatial parallel manipulators.

Degrees of freedom d	Sum of all joint freedoms $\sum_i d_i$		Connectivity listing C_k, $k = 1, 2, 3\ldots$
2	8		4,4
			5,3
			6,2
3	15		5,5,5
			6,5,4
			6,6,3
4	22		6,6,5,5
			6,6,6,4
			1,2,3
			2,2,2
6	$m = 3$	18	6,6,6
	$m = 6$	36	6,6,6,6,6,6

Let the connectivity C_k of the kth limb be defined as the DOF associated with all joints on that limb. Then

$$\sum_{k=1}^{m} C_k = \sum_{i=1}^{j} d_i \tag{5}$$

Substituting equation (3) into equation (5), and eliminating l by making use of equation (4), the following is obtained

$$\sum_{k=1}^{m} C_k = (\lambda + 1)d - \lambda. \tag{6}$$

To ensure proper mobility and controllability of the moving platform, the connectivity of each limb should not be greater than the motion parameter nor less than the DOF of the moving platform, i.e.

$$d \leqslant C_k \leqslant \lambda. \tag{7}$$

Equations (1), (4), (6) and (7) completely characterize the structural topology of all parallel manipulators except that of six-DOF parallel manipulators.

Now consider the case of six-DOF manipulators. Considering symmetry in actuation, the number of limbs in the case of six-DOF manipulators vary between 2, 3 and 6 (refer to tables 1). Actuation of the base proximal joints allows passive joint groups to be placed at the end of the branches, reducing the manipulator mass. A spherical joint in the branch structure renders the branch kinematically simple. There are three actuators in each limb for a two-legged, six-DOF parallel manipulator. This mechanism cannot, however, employ passive spherical joints at the leg ends since the end-effector would no longer be fully constrained. Thus, in the enumeration here only three- and six-legged manipulators are considered. Equations characterizing the structural topology of six-DOF manipulators are

$$d = \lambda(n - j - 1) + \sum_i d_i \tag{8}$$

$$m = L + 1 \tag{9}$$

$$\sum_{k=1}^{m} C_k = d + \lambda(m - 1) \tag{10}$$

$$d \leqslant C_k \leqslant \lambda \tag{11}$$

$$m = 3, 6 \tag{12}$$

Planar reconfigurable parallel manipulators. For planar reconfigurable manipulators, $\lambda = 3$. Let revolute and prismatic joint types be the available joint types. Then all the revolute joint axes must be perpendicular to the plane of motion and the prismatic joint axes must lie on the plane of motion.

- Planar two-DOF reconfigurable manipulators. Equation (6) yields

$$\sum_{k=1}^{2} C_k = 5.$$

  A simple combinatorial analysis as done by Tsai (2000) yields the following possible closed-loop, five-bar linkages: RRRRR, RRRRP, RRRPP and RRPRP. Considering the weight of prismatic joint modules and the symmetry of legs, the candidate two-DOF reconfigurable planar parallel manipulators can have RRRRR and PRRRP configurations (figure 6).
- Planar three-DOF manipulators. For planar three-DOF parallel manipulators, substituting $\lambda = 3$ and $d = 3$ into equation (6), gives

$$C_1 + C_2 + C_3 = 4d - 3 = 9 \tag{13}$$

  Furthermore, equation (7) reduces to

$$3 \leqslant C_k \leqslant 3 \tag{14}$$

  Hence, the connectivity of each limb should be equal to three. That is, each limb has three DOF in its

joints. Using revolute and prismatic joints as the available kinematic pairs, seven possible limb configurations can be identified: RRR, RRP, RPR, PRR, RPP, PRP and PPR. The PPP combination is rejected because it does not permit rotation of the end-effector. From a potential $7^3 = 343$ possible planar three-DOF parallel manipulators, over seven configurations are chosen. Considering the weight of prismatic joint modules, candidate limb configurations are: RRR, PRR and RPR (figure 7). A prototype of the RRR-type parallel manipulator, built in the current authors' laboratory, (figure 7(a)) and a conceptual PRR (figure 7(b)) and RPR-type (figure 7(c)) parallel manipulators are shown.

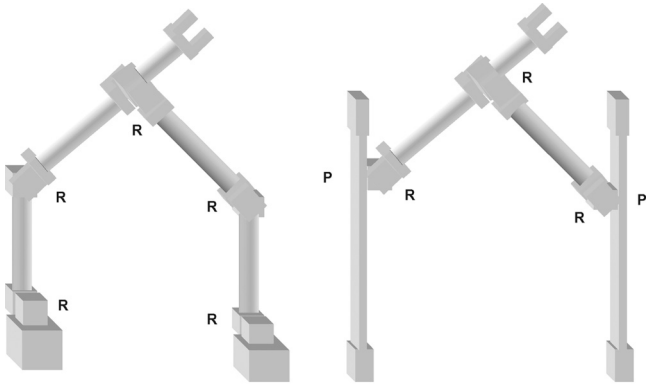

(a) RRRRR-type (b) PRRRP-type

Figure 6. Five-bar reconfigurable parallel manipulators: (a) RRRRR-type; (b) PRRRP-type.

Spatial parallel manipulators. Table 2 shows the classification of spatial parallel manipulators according to their DOF and connectivity listings.

The number of limbs incorporated in each limb can be an arbitrary integer as long as the sum of all joints of freedom is equal to the required connectivity. The maximum number of links occur when all the joints are one-DOF joints. It can be seen that there is no leg-symmetry in the case of 4 and 5-DOF manipulators. Therefore, in this discussion, only three-, and six-DOF manipulators are enumerated.

- Three-DOF translational platforms. Considering the joint symmetry, the (5,5,5) connectivity (shown in table 2) is the only feasible solution. Taking into account the available types of joint modules (revolute, prismatic, universal and spherical), thirteen feasible types of limbs can be listed. For each type of limb listed in table 3, the first digit denotes the number of joints, the second digit denotes the

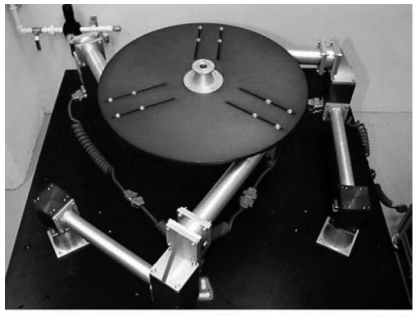

(a) A reconfigurable RRR-type planar manipulator

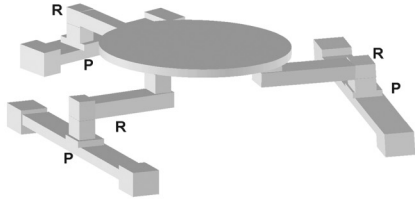

(b) Conceptual reconfigurable PRR-type planar manipulator

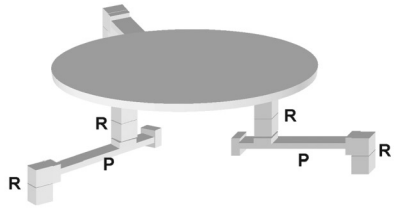

(c) Conceptual reconfigurable RPR-type planar manipulator

Figure 7. Three-DOF planar mechanisms: (a) reconfigurable RRR-type planar manipulator; (b) conceptual reconfigurable PRR-type; (c) conceptual reconfigurable RPR-type planar manipulator.

number of two-DOF joints and the third digit denotes the number of three-DOF joints. Since it is preferable to have a ground-connected revolute or prismatic joint, SRR, SRP, URU, UUR and UUP configurations are eliminated.

As a spherical joint cannot provide any constraint on the rotation of the moving platform, the entire type-201 limb configurations are eliminated from further discussion. Owing to the weight of the prismatic joint, it should be mounted at the first or second joint from the base. Also for a parallel manipulator design, the actuators should be placed close to the base. Thus the possible configurations are RUU, PUU and UPU. To achieve pure translation, the axes of the two universal joints must be arranged in a special configuration. The two inner revolute joint axes of the U–U pair must be parallel to each other. The prismatic joint of the PUU limb can be directed along any direction. The base-connected revolute joint of the RUU limb must be parallel to the two outer joint axes of the U–U pairs. Figure 8 shows the schematic diagram of RUU- and PUU-type configurations. Other possible reconfigurable configurations with available joint modules are RRS, RPS and PRS (shown in figure 9). Three-DOF spatial parallel manipulators having all-rotational DOFs include agile eye (RRR).

Table 3. Limb configuration of spatial three-DOF manipulators.

Type	Kind
201	RRS,RSR,RPS,RSP,PSR,PRS,SPR,PPS,PSP,SPP
120	UPU,RUU,PUU

- Six-DOF parallel manipulators. Considering the leg-symmetry, the discussion here is limited to parallel manipulators that have three or six legs. Table 1 shows the enumeration scheme for a class of parallel robots with a six-DOF, non-redundant, topological structure (Podhorodeski and Pittens 1994) having three and six legs.
- Three-legged parallel manipulators. Considering three legs of a parallel manipulator having six-DOF and symmetry in actuation, the 2-2-2 actuation scheme is chosen (table 1). Hence, there are two actuators in each limb of the parallel manipulator. The connectivity of each limb is six (table 2). Thus, type-301 is the only possible limb type (table 3), i.e. in each limb there are three one-DOF joints out of which there are two active and one passive spherical joint. It is preferred that actuator joints are not the end joints of a limb. Also if the spherical joint is the end joint of the limb, the kinematics are simple. Thus in this design, the spherical joint is chosen as the end joint and the three one-DOF joints can be any combination between revolute and prismatic joints. Owing to the weight and actual construction, prismatic joint modules are mounted close to the base and only one prismatic joint should be used per leg. The possible limb configurations can only be RRRS, PRRS and RPRS type. Figures 10 and 11 show three six-DOF three-legged (2-2-2) parallel manipulators that have been constructed in the current authors' laboratory.
- Six-legged parallel manipulators. For six-legged parallel manipulators, the connectivity listing is (6,6,6,6,6,6) (refer to table 2). In order to minimize the number of joints in a leg, the 111 type of limb is chosen, which means that each limb consists of one of each of one-, two- and three-DOF joints. There are six feasible limb configurations with the available

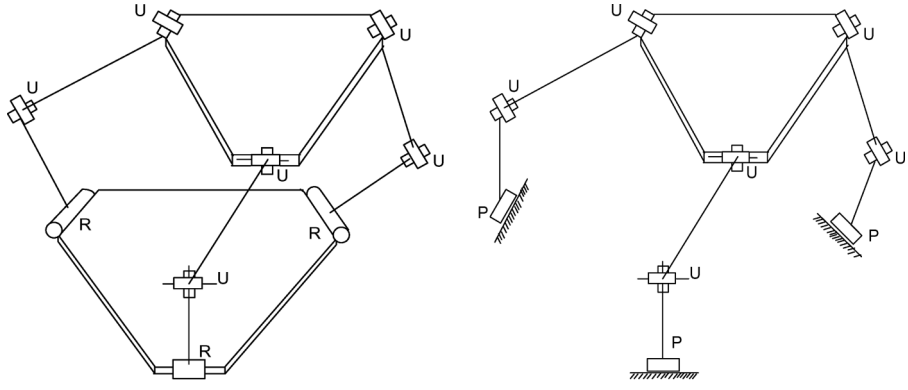

(a) *RUU*-type spatial three-DOF translational manipulator

(b) *PUU*-type spatial three-DOF translational manipulator

Figure 8. Spatial three-DOF translational mechanisms (Tsai 2000).

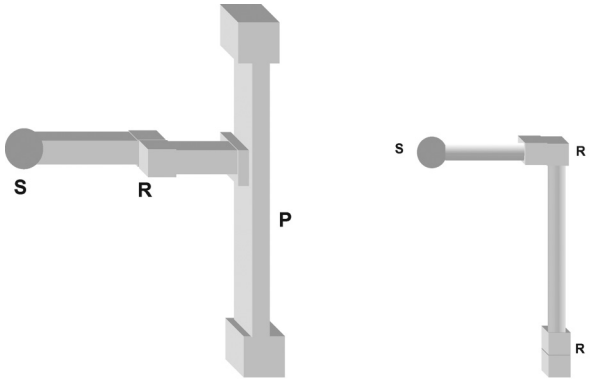

(a) *PRS*-type leg of spatial three-DOF manipulator

(b) *RRS*-type leg of a spatial three-DOF manipulator

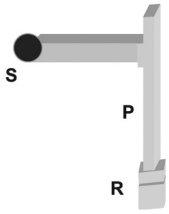

(c) *RPS*-type leg of a spatial three-DOF manipulator

Figure 9. Spatial three-DOF mechanisms.

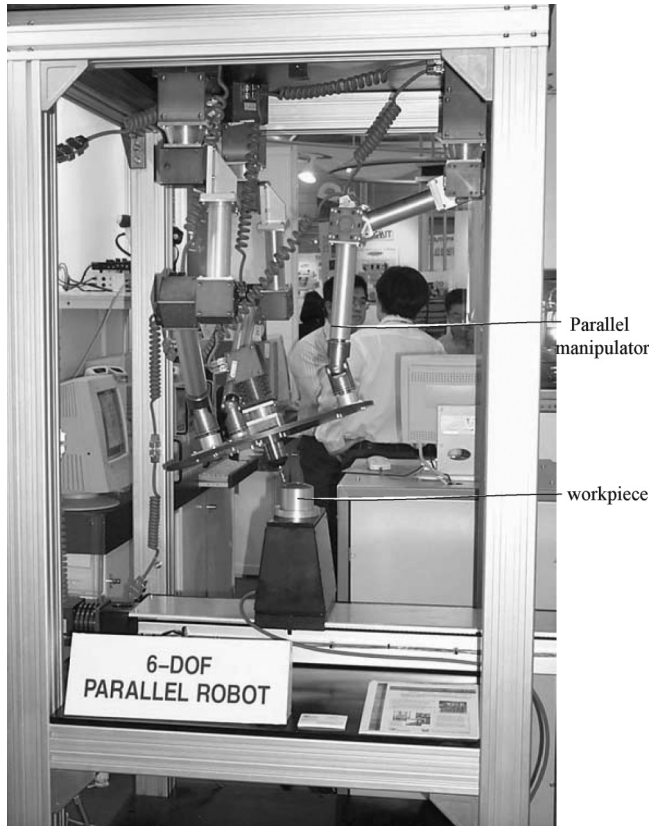

Figure 10. Workpiece and six-DOF RRRS-type three-legged parallel manipulator.

revolute, prismatic, universal and prismatic joints: RUS, RSU, PUS, PSU, SPU, and UPS; these are discussed in detail in Tsai (2000).

All manipulators, determined by enumeration, constitute the reconfigurable robot assembly database (table 4). Note that as the module inventory grows and the functional requirements are changed, this database will change accordingly.

3.4. Topology selection based on task analysis

To select a type of parallel mechanism for a specific task, task analysis is required. This analysis involves knowing the DOF associated with the task, the types of DOF, the constraints on the mechanism like joint limitations, maximum torque limits of the joints, maximum and minimum workspace, singularities, etc. and performance criterion like stiffness, accuracy, condition number. A wide knowledge of the types of mechanisms and the kinds of tasks they can perform is very helpful for the designer. A `TaskToRobot` map solves this purpose and helps the designer to select type(s) of mechanism(s) for the specific task at hand. In section 3.2, parallel manipulators are enumerated based on the number of DOF (Tsai 2000 and Merlet 2000) of the end-effector. The DOF plays an important role in the analysis of the task and in the enumeration of mechanisms. Therefore, type(s) of mechanism(s) is (are) selected based on the DOF associated with the task. For this purpose, the `TaskToRobot` map (table 5) is proposed for the designer to choose a particular kind of parallel mechanism for a task. This mapping is based on the knowledge of the designer, which can be updated from time to time depending upon the adaptability of a particular mechanism for tasks requiring certain DOF. Table 5 is constructed based on information collected from different sources (Angeles 1997, Merlet 2000 and Dasgupta and Mruthyunjaya 2000).

4. Parameter-determination stage

With the help of the `TaskToRobot` map, one or a few particular mechanisms are selected for a specific task. An optimization technique is then followed to determine the dimensions for each of the selected manipulators to satisfy the task requirements, and the one with the optimal value of objective function is selected as the optimal parallel manipulator. For demonstration, three-legged parallel manipulators are focused on here. The task is specified in terms of the coordinates of the task points, the trajectory to

(a) RPRS-type leg-structure (b) RRRS-type leg-structure

Figure 11. Two different six-DOF, three-legged reconfigurable parallel manipulators.

Table 4. Reconfigurable robot assembly database.

		Reconfigurable parallel manipulators	
Degrees of freedom		No. of legs	Configuration of each leg
2		2	RRR
			PRR
3 (Planar)		3	RRR
			PRR
3 (Spatial)	All trans.	3	RUU
			PUU
			UPU
	Trans. + rot.	3	PRS
			RRS
			RPS
	All rot.	3	RRR
6		3	RRRS
			PRRS
			RPRS
		6	UPS

be followed, the type of end-effectors used, external forces and torques, operating space constraints (volume and area available) on the mechanism, etc.

4.1. *Task*

The task under consideration is specified by translational and rotational accuracy, reachable workspace of the task, type of workpiece material, maximum and minimum force and torque required along different axes. Other constraints include safety limit of joint torques, joint angle limitations of actuators, etc.

4.2. *Design parameters with effect of actuation scheme*

The design parameters of a three-legged parallel manipulator include dimensions of the base platform, the end-effector platform and the link lengths. In this work, the actuation scheme is also considered as a design variable. The actuation scheme is an important aspect in the design of a parallel manipulator because location of the actuators determines the forms of the manipulator Jacobians, i.e. when the actuation scheme changes, the form of the manipulator Jacobian matrices changes while the configuration of the parallel manipulator remains the same.

For example, consider the RRRS-type three-legged parallel manipulator as shown in figure 10. The velocity

Table 5. Look-up table to map tasks onto parallel manipulators.

S/N	Degrees of freedom		Example of Tasks	Possible PKMs	
				No. of legs	Config. of each leg
1		Rot. + Rot.	Rolling		RRR
	2	Trans. + Rot.		2	PRR
		Trans. + Trans.			
2	3 (Planar)		Planar positioning devices	3	RRR
					PRR
			Pick-and-place (light load)		
		Trans.	Food industry for manipulation		RUU
3	3 (spatial)	Trans.	Microscope stand (medical field)	3	PUU
			Positioning devices		
			Insertion, peg-in-a-hole		
		Trans. + Rot.	Balancing a spaceship	3	PRS
			Micromanipulation		RRS
			Active head for endoscope		
			Light machining task	3	RRRS
					PRRS
			Manipulation of ship components		
			Ultra-fast assembly		
			Coordinate measuring machine		
			Electronic component assembly		
			Flight simulators		
		3 Trans.	Fine positioning devices		
			Structural vibration control		
			Docking devices		
4	6	+	Aerial orientation mechanism	6	UPS
			Aerial pointing devices		
			Micro-gravity surrounding		
		3 Rot.	Study of impact		
			Medical surgery		
			Molecular exploration		
			Test-bed for intervertebral motion		
			Part handling and spot welding		
			Support for a painting tube		
			Six-axis milling machines		

relationship between the end-effector and that of joints is given by

$$A\mathbf{V} = B\dot{\boldsymbol{\theta}}_a \tag{15}$$

where

$$A = \begin{bmatrix} \mathbf{a}_{11} \\ \mathbf{a}_{12} \\ \mathbf{a}_{21} \\ \mathbf{a}_{22} \\ \mathbf{a}_{31} \\ \mathbf{a}_{32} \end{bmatrix} \tag{16}$$

and

$$B = \begin{bmatrix} b_{11} & 0 & 0 & 0 & 0 & 0 \\ 0 & b_{12} & 0 & 0 & 0 & 0 \\ 0 & 0 & b_{21} & 0 & 0 & 0 \\ 0 & 0 & 0 & b_{22} & 0 & 0 \\ 0 & 0 & 0 & 0 & b_{31} & 0 \\ 0 & 0 & 0 & 0 & 0 & b_{32} \end{bmatrix} \tag{17}$$

Here $\mathbf{a}_{ij}$ and b_{ij} for $i=1$, 2, 3 denote the labels of the three legs and $j=1$, 2 or 3, denoting the labels of the

actuator joints in the leg; $\mathbf{V}$ and $\dot{\boldsymbol{\theta}}_a$ denote the velocities of the end-effector and the active joints respectively. When the first two joints of each leg of this class of manipulators are actuators, $\mathbf{a}_{11}$ and $\mathbf{a}_{12}$ of forward Jacobian matrix (matrix A) have the form as given in equation (18)

$$\mathbf{a}_{11} = \left[\left\{ \left([I - \hat{p}_{14}] s_{12} \right) \times \left([I - \hat{p}_{14}] s_{13} \right) \right\}^T - \left\{ \left(\left([I - \hat{p}_{14}] s_{12} \right) \times \left([I - \hat{p}_{14}] s_{13} \right) \right) \times \mathbf{p}_{14} \right\}^T \right]$$

$$\mathbf{a}_{12} = \left[\left\{ \left([I - \hat{p}_{14}] s_{11} \right) \times \left([I - \hat{p}_{14}] s_{13} \right) \right\}^T - \left\{ \left(\left([I - \hat{p}_{14}] s_{11} \right) \times \left([I - \hat{p}_{14}] s_{13} \right) \right) \times \mathbf{p}_{14} \right\}^T \right] \quad (18)$$

where s_{ij} is the twist associated with jth joint of ith leg and p_{i4} is the position vector joining origin of the base platform to the end-joint of ith leg. However, these terms change to equation (19) when the actuators are placed at the first and the third joints

$$\mathbf{a}_{11} = \left[\left\{ \left([I - \hat{p}_{14}] s_{12} \right) \times \left([I - \hat{p}_{14}] s_{13} \right) \right\}^T - \left\{ \left(\left([I - \hat{p}_{14}] s_{12} \right) \times \left([I - \hat{p}_{14}] s_{13} \right) \right) \times \mathbf{p}_{14} \right\}^T \right]$$

$$\mathbf{a}_{13} = \left[\left\{ \left([I - \hat{p}_{14}] s_{11} \right) \times \left([I - \hat{p}_{14}] s_{12} \right) \right\}^T - \left\{ \left(\left([I - \hat{p}_{14}] s_{11} \right) \times \left([I - \hat{p}_{14}] s_{12} \right) \right) \times \mathbf{p}_{14} \right\}^T \right] \quad (19)$$

This change in the manipulator Jacobians fundamentally changes the performance of the parallel manipulators. The effect of actuation scheme on the performance criteria of parallel manipulators is discussed in section 4.4.

4.3. *Objective function*

The objective function is to evaluate the goodness of a configuration selected. There are local and global measures to evaluate the suitability of a parallel manipulator. Local measures for a parallel manipulator are the criteria or functions describing the performance of a parallel manipulator at a small zone of the workspace, whereas the global measures describe the performance spreading over the entire workspace. Stiffness analysis, accuracy analysis, the condition number and manipulability are considered as the local measures, whereas the workspace volume is a measure of global performance of the manipulator. Many local measures may be converted to global measures by evaluating the over the entire workspace. To determine such global measures, however, is computationally very intensive.

A task-based design methodology for reconfigurable parallel manipulators mainly concerns the performance of the manipulator for a specific task: it is not meant for generic tasks or a large variation of tasks. Hence, local measures of the manipulator play a more important role than the global measures for reconfigurable parallel manipulators. The objective function of the entire task is defined as raised to the reciprocal of the number of points of the product of individual condition index at each of the task points, i.e. the objective function is expressed as

$$\left(\prod_{i=1}^{n} 1/c_i \right)^{1/n}$$

where c_i, $i = 1, 2, \ldots, n$ denotes the condition number at ith task point and condition index is the reciprocal of condition number. Using the product of condition indices enables the singularity points at the task points to be deduced easily.

The condition number is used as the evaluation criterion because it appears to be the most suitable index from the perspective of singularity avoidance and kinematic accuracy. In addition, the condition number is directly related to the isotropic or robust design of parallel manipulators and to the stiffness of the parallel manipulator. A well-distributed stiffness ellipsoid represents a good distribution of stiffness at the task point and a better condition number. The condition number (c) of the Jacobian matrix based on matrix 2-norm is given as the ratio of largest to smallest singular values. Since the minimum value of the condition number is 1 and the maximum value is infinity, the reciprocal of the condition number, called the 'conditioning index', is chosen, i.e.

$$\frac{1}{c} = \frac{\sigma_{\min}}{\sigma_{\max}} \quad (20)$$

where $\sigma_{\min}$ and $\sigma_{\max}$ are the smallest and largest singular values of the Jacobian matrix, respectively.

The relationship between the velocity of the end-effector to that of the joints for a parallel manipulator is given by equation (15). It can also be written as

$$\dot{\theta} = J\dot{\mathbf{X}} \quad (21)$$

$$\text{or} \quad \Delta\theta = J\Delta\mathbf{X} \qquad \text{in difference form} \quad (22)$$

where $J = B^{-1} A$ and B is a diagonal matrix.

4.4. *Performance constraints*

The performance constraints are defined to ensure the feasibility of a robot configuration while performing the given task. The constraints considered here are:

1. reachability,
2. joint torque limitations.

The *reachability constraint* is used to inspect whether all the task points are inside the reachable workspace of the parallel manipulator. If this constraint is satisfied then the parallel manipulator is able to perform the given task kinematically. To study the reachability constraint, the problem is transformed into an inverse kinematic problem. Chen and Gao (2001) proposed a closed-form inverse kinematics solver for reconfigurable serial robots. Since a parallel manipulator consists of several open-loop chains, this solver is used to determine if the inverse kinematics of each leg exists at each of the task points. If all the legs satisfy the inverse kinematics, the reachability constraint of the manipulator is satisfied. The reachability constraint of a three-legged parallel manipulator having nine one-DOF joint modules is given by

$$\theta_{\min_i} \leqslant \theta_i \leqslant \theta_{\max_i} \qquad (i = 1, 2, \ldots, 9), \tag{23}$$

where $\theta_{\min_i}$ and $\theta_{\max_i}$ are the minimum and maximum joint limits of the ith joint module.

The *joint torque limitation constraint* is defined to determine whether any of the actuator joints are unable to generate enough torque at any task point. Here only the static characteristics are considered. The relationship between joint torques and the end-effector force is given as follows

$$\tau_i = J^{-T} F \qquad (i = 1, 2, \ldots, 6) \tag{24}$$

Normally for calculation purposes, only the Jacobian matrix (J^{-T}) is considered. In the case of a reconfigurable system, since each module has a predefined joint torque limit, the joint torque limitation constraint for a parallel manipulator having six actuator modules is given by

$$\tau_i \leqslant b_i \qquad (i = 1, 2, \ldots, 6) \tag{25}$$

where b_i is the limit torque that can be generated in ith actuator module.

4.5. *Effect of the actuation scheme*

To study the effect of the actuation scheme on the performance criteria of a parallel manipulator, consider the RRRS-type three-legged parallel manipulator as shown in figure 10. The performance criteria studied are condition number and the ratio of the maximum and minimum forces on the end-effector. These performance measures are functions of the manipulator Jacobian matrix. As discussed in section 4.2, when the actuation scheme changes the form of the manipulator Jacobian matrix also changes.

Two types of actuation schemes are considered: (1,2)-actuation scheme (read as one-two actuation scheme, i.e. first and second joints from the base are active) and (1,3)-actuation scheme (first and third joint from the base are active). The (2,3)-actuation scheme is not considered because it has forward singularities along the vertical line joining the centre points of the platform and the end-effector (Dash *et al*. 2001). The results are plotted and show how the actuation scheme affects the translational accuracy of the parallel manipulator at different heights selected. From figure 12, it is observed that when height (distance along the Z direction) is 300 mm, the condition number with (1,2)-actuation scheme is better than that of (1,3)-actuation scheme. However, when the height changes to 900 mm, the (1,3)-actuation scheme has a larger condition number. The changeover takes place within 500 mm to 700 mm of the height. Ideally, the ratio of maximum to minimum forces should be 1 so that the design can be isotropic. In figure 13, it is observed that when the height is 300 mm and 500 mm, this ratio for the (1,2)-actuation scheme is lower than of (1,3)-actuation scheme (which is desired). However, at the height of 900 mm, the (1,3)-actuation scheme performs better than (1,2)-actuation scheme. The changeover takes place at a height of 700 mm. The observations can be summarized as follows.

1. The manipulator performs well at a lower position (closer to the base) when there is a (1,2)-actuation scheme.
2. The manipulator performs well at a higher position with a (1,3)-actuation scheme.
3. The changeover is dependent upon the individual expression of these performance measures, i.e. the changeover for condition number is different from that of accuracy because both are different functions of the manipulator Jacobians. Thus, it is essential to include the actuation scheme as a design variable.

The objective of this optimization algorithm is to determine the optimal dimensions and actuation scheme of a class of three-legged parallel manipulators for a specific task. This class of parallel manipulators have nine one-DOF joints, six of them are active joints. For simplicity, symmetric leg design is assumed. A task for this parallel manipulator is defined by n-task points. The optimization algorithm solves a non-linear constrained optimization problem defined as follows

$$\text{maximize} \left(\prod_{i=1}^{n} \frac{1}{c_i} \right)^{1/n}$$

subjected to

$$\theta_{\min_j} \leqslant \theta_j \leqslant \theta_{\max_j} \ (j = 1, 2, \ldots, 9) \text{ (reachability constraint)}$$

$$\tau_j \leqslant b_j \ (j = 1, 2, \ldots, 6) \text{ (joint torque limitation constraint)}$$

where c_i for $i = 1, 2, \ldots, n$ denotes the condition number respectively and θ_j, and τ_j denote the joint displacement and torque in the jth joint, respectively.

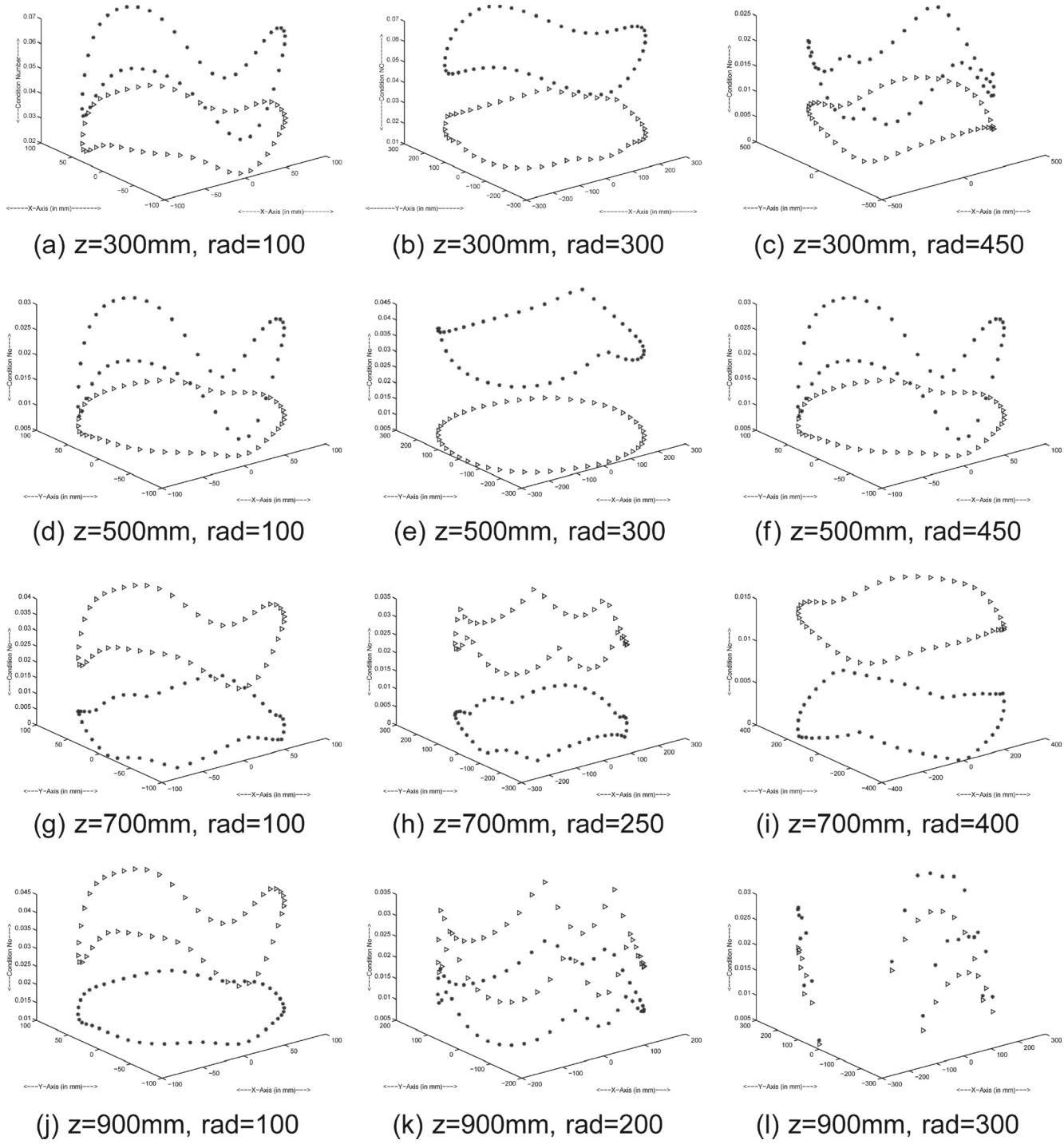

Figure 12. Values of the condition number at different heights and radii ($\star$: (1,2)-actuation scheme, $\triangleright$: 13 actuation scheme).

An initial configuration of the parallel manipulator, the coordinates of the task points, the forces acting on the end-effector at these points and the joint torque limits are the inputs to this optimization algorithm. The objective function and the constraints are nonlinear. The design variable includes continuous and discrete variables: link dimensions of the parallel manipulator are continuous variables whereas the actuation scheme is a discrete variable. Therefore, the link lengths are bound by a minimum and maximum lengths and the optimal value can vary between these limits in a continuous manner. The actuation scheme is discrete, i.e. it can be either one of the

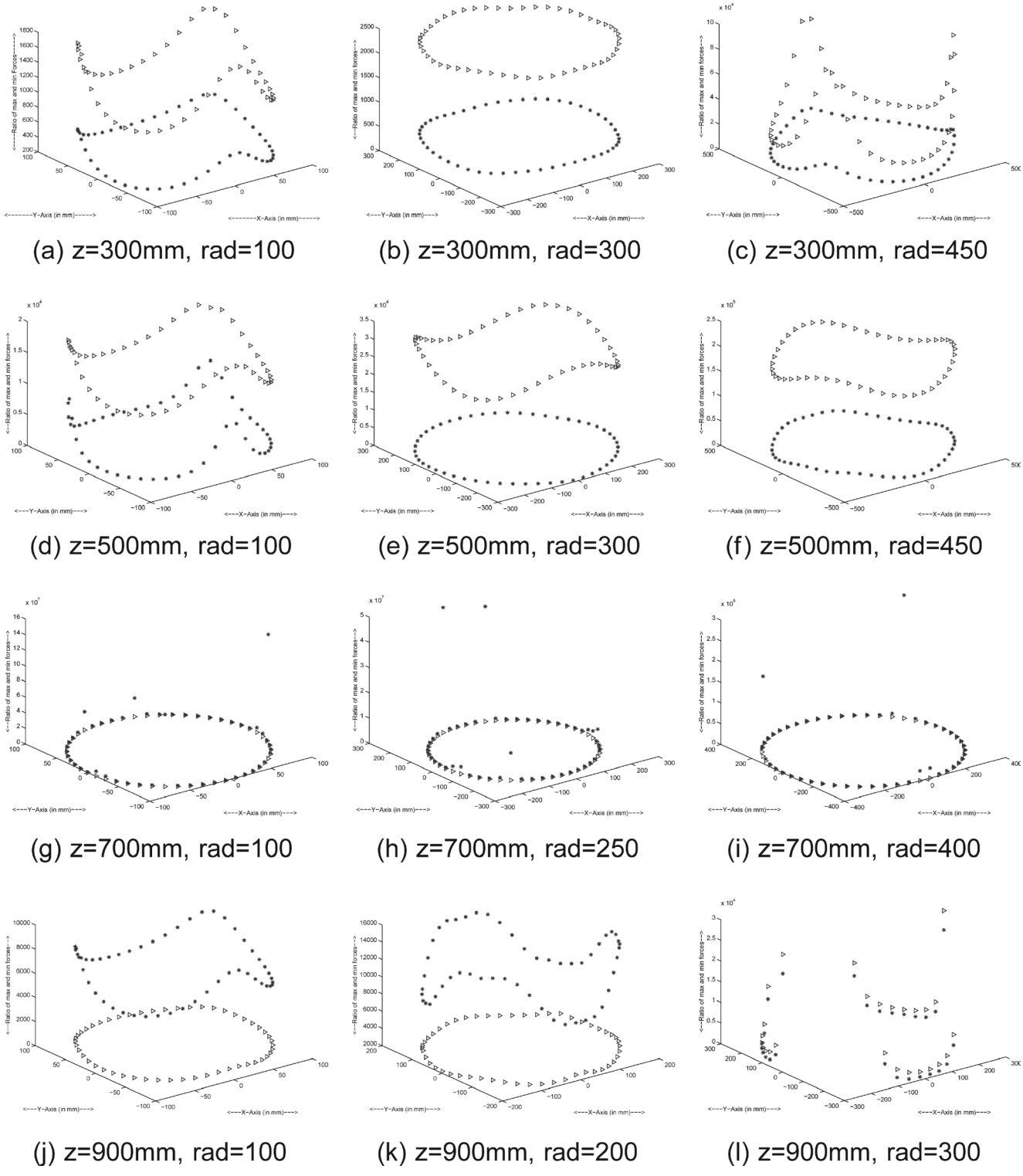

Figure 13. Ratio of maximum and minimum forces at different heights and radii ($\star$: (l,2)-actuation scheme, $\triangleright$: 13 actuation scheme).

many possible order of actuations. The entire optimization procedure is shown in figure 14. In each iteration, the objective function is calculated for the total number of enumerated actuation schemes and the largest value among them is chosen as the value of the objective function for that iteration.

For this constrained optimization, SIMPS optimization algorithm is used (Bunday and Garside 1987). SIMPS is an iterative method. It is stable and robust, although it is less efficient than the steepest-descent-type of algorithms. Although the steepest descent methods, such as the quasi-Newton method and the Powell method, converge to a minimum fast, the solution obtained is not stable and is not always within the limits of the constraint parameters. However, SIMPS the employing of the Simplex method is always able to find an acceptable and valid solution. In this search method, the number of points in the initial *simplex* is much less compared with that in the evolutionary optimization method. This reduces the number of function evaluations required in each iteration.

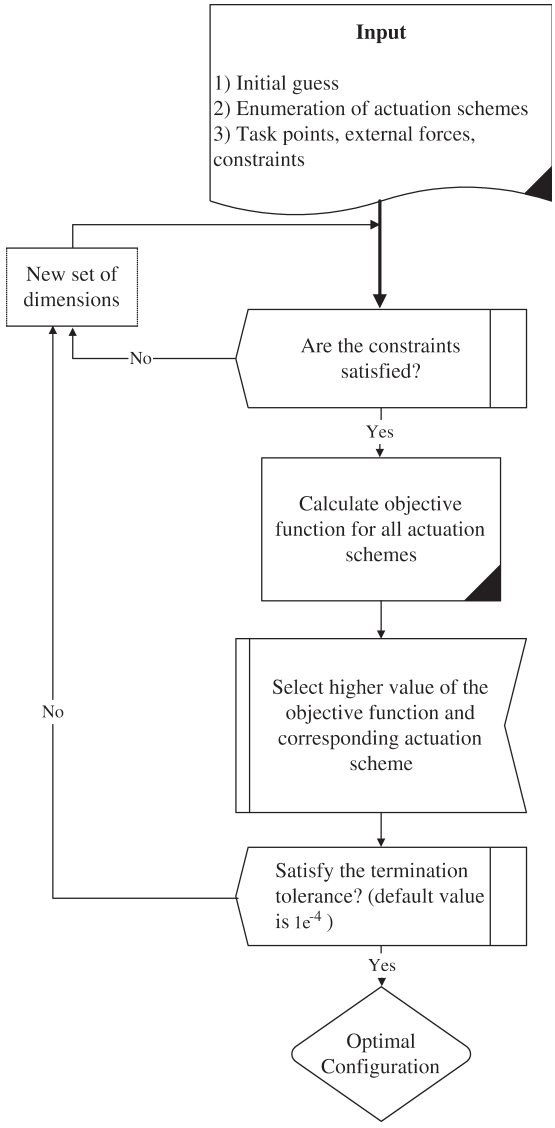

Figure 14. The optimum design procedure.

5. Case study

Consider a light milling task to make a spherical shaped object made of mild steel. The end-effector is a milling cutter of radius 50 mm having twenty teeth. The velocity of the table is 15 mm/min and the cutter rotates at 10000 r/min. The depth of cut of 1 mm is used. A diagram of the set up is shown in figure 10.

The poses of the five task points are:

$$T1 = \begin{bmatrix} 1 & 0 & 0 & 0 \\ 0 & 1 & 0 & 0 \\ 0 & 0 & 1 & 0.94 \\ 0 & 0 & 0 & 1 \end{bmatrix};$$

$$T2 = \begin{bmatrix} 1 & 0 & 0 & 0 \\ 0 & \cos\beta & \sin\beta * 0.08 * \sin\beta & 0.08 * \sin\beta \\ 0 & -\sin\beta & \cos\beta & 940 - 80 * (1 - \cos\beta) \\ 0 & 0 & 0 & 1 \end{bmatrix};$$

$$T3 = \begin{bmatrix} \cos\beta & 0 & \sin\beta & 0.08 * \sin\beta \\ 0 & 1 & 0 & 0 \\ -\sin\beta & 0 & \cos\beta & 940 - 80 * (1 - \cos\beta) \\ 0 & 0 & 0 & 1 \end{bmatrix};$$

$$T4 = \begin{bmatrix} 1 & 0 & 0 & 0 \\ 0 & \cos\beta & -\sin\beta & -80 * \sin\beta \\ 0 & -\sin\beta & \cos\beta & 940 - 80 * (1 - \cos\beta) \\ 0 & 0 & 0 & 1 \end{bmatrix};$$

$$T5 = \begin{bmatrix} \cos\beta & 0 & -\sin\beta & -80 * \sin\beta \\ 0 & 1 & 0 & 0 \\ \sin\beta & 0 & \cos\beta & 940 - 80 * (1 - \cos\beta) \\ 0 & 0 & 0 & 1 \end{bmatrix}$$

where $\beta = \pi/10.0$. Figure 15 shows the three views of the workpiece and the co-ordinates of the task points.

The force and torque analysis of this task (Ghosh and Mallik 1986), gives the values of external torques acting at the five task points as shown in table 6. Other specifications of the task are given in table 7.

In the structure-determination stage, the desired parallel manipulator chosen is a three-legged reconfigurable parallel manipulator. Here the RRRS-type three-legged parallel manipulator is preferred to the RPRS-type parallel manipulator because the prismatic modules are bulky and heavy (the weight of the prismatic module is 15 kg and that

of a rotary module is 3.8 kg.); it is also costly compared to the revolute ones. The overall weight of the mechanism will be reduced.

For the parameter optimization, six design variables are selected including the actuation scheme. The design variables are:

1. base radius ($L11$),
2. length of the link connecting base joint to first joint ($H12$),
3. length of the link connecting first joint to second joint ($H13$),
4. length of the link connecting second joint to third joint ($H14$),
5. platform radius ($L12$) (refer to figure 16),
6. actuation scheme.

The actuation scheme is enumerated as follows: there are two actuators on each leg. For a symmetric actuation scheme, the arrangement of two actuators in each of the three legs is identical. Thus, possible actuation schemes are (1,2) (actuators are placed at first and second joint from base), (1,3) (actuators at first and third joint) and (2,3) (actuators at second and third joint). Out of these three, the (2,3)-actuation scheme is not considered because it has forward singularities along a vertical line connecting the centre points of the base and the mobile platform.

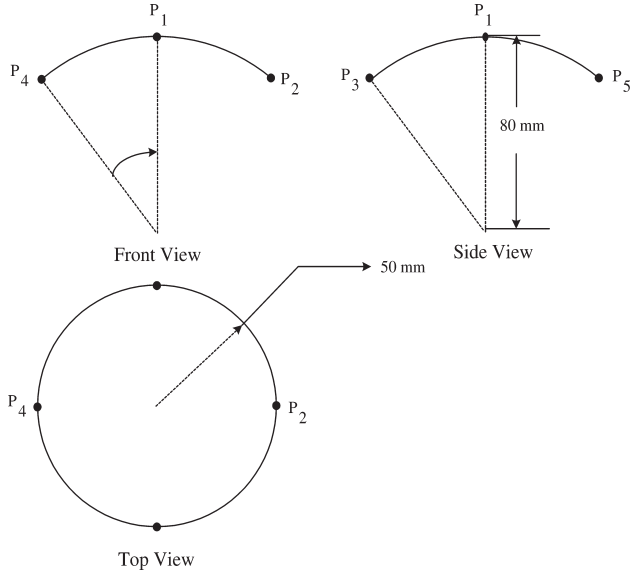

Figure 15. Three views of the workpiece and coordinates of the task points.

The optimization problem can be stated as

$$\text{maximize} \left(\prod_{i=1}^{5} \frac{1}{c_i} \right)^{1/5}$$

subjected to constraints

$$\theta_{\min_j} \leqslant \theta_j \leqslant \theta_{\max_j} \quad (j = 1, 2, \ldots, 9) \text{ (reachability constraint)}$$

$$\tau_j \leqslant b_j \quad (j = 1, 2, \ldots, 6) \text{ (joint torque limitation constraint)}$$

where c_i denotes the condition number at ith task point, and θ_j, and τ_j denote the joint displacement and torque in the jth joint, respectively. There are a total of nine one-DOF joints, six are active and three are passive. The motion range of each of the passive joints is $[0 \sim 2\pi]$ and that of an actuator module is $[-\pi \sim \pi]$. The torque limit of each active joint is 49 Nm (determined by the product specifications).

The initial parameter set is given as $L11 = 0.35$, $H12 = 0.215$, $H13 = 0.295$, $H14 = 0.3325$, and $L12 = 0.1955$ (all dimensions are in meters). This the initial assembly configuration of the parallel manipulator under consideration. The other kinematic parameters chosen are

$$T_{B,B_{10}} = \begin{bmatrix} \frac{1}{2} & -\frac{\sqrt{3}}{2} & 0 & -0.175 \\ \frac{\sqrt{3}}{2} & \frac{1}{2} & 0 & -0.175\sqrt{3} \\ 0 & 0 & 1 & 0.045 \\ 0 & 0 & 0 & 1 \end{bmatrix};$$

$$T_{B,B_{20}} = \begin{bmatrix} -1 & 0 & 0 & 0.350 \\ 0 & -1 & 0 & 0 \\ 0 & 0 & 1 & 0.045 \\ 0 & 0 & 0 & 1 \end{bmatrix};$$

Table 6. Force and torque distribution at different task points.

	F_x	F_y	F_z	τ_{xy}	τ_{yz}	τ_{zx}
F_1	4.89	4.89	0	0	0	0.0546
F_2	4.89*cosβ	4.89*cosβ	1.96	0.0546*sinβ	0	0.0546*cosβ
F_3	4.89*cosβ	4.89*cosβ	1.96	0.0546*sinβ	0	0.0546*cosβ
F_4	4.89*cosβ	4.89*cosβ	1.96	0.0546*sinβ	0	0.0546*cosβ
F_5	4.89*cosβ	4.89*cosβ	1.96	0.0546*sinβ	0	0.0546*cosβ
F_6	4.89*cosβ	4.89*cosβ	1.96	0.0546*sinβ	0	0.0546*cosβ

$$T_{B,B_{30}} = \begin{bmatrix} \frac{1}{2} & \frac{\sqrt{3}}{2} & 0 & -0.175 \\ -\frac{\sqrt{3}}{2} & \frac{1}{2} & 0 & 0.175\sqrt{3} \\ 0 & 0 & 1 & 0.045 \\ 0 & 0 & 0 & 1 \end{bmatrix}; \; T_{B_{i0},B_{i1}} = \begin{bmatrix} 1 & 0 & 0 & 0 \\ 0 & 1 & 0 & 0 \\ 0 & 0 & 1 & 0 \\ 0 & 0 & 0 & 1 \end{bmatrix};$$

$$T_{B_{i1},B_{i2}} = \begin{bmatrix} 0 & 1 & 0 & 0 \\ 0 & 0 & 1 & 0 \\ 1 & 0 & 0 & 0.215 \\ 0 & 0 & 0 & 1 \end{bmatrix}; \; T_{B_{i2},B_{i3}} = \begin{bmatrix} 1 & 0 & 0 & 0.295 \\ 0 & 1 & 0 & 0 \\ 0 & 0 & 1 & 0 \\ 0 & 0 & 0 & 1 \end{bmatrix};$$

$$\bar{p}_i'' = \begin{bmatrix} 0.3325 \\ 0 \\ 0 \\ 1 \end{bmatrix}$$

where $i = 1, 2, 3$ stands for each leg. The twist coordinates of the screw axes are $s_{11} = s_{12} = s_{13} = s_{31} = (0, 0, 0, 0, 0, -1)$; $s_{21} = s_{22} = s_{23} = s_{32} = s_{33} = (0, 0, 0, 0, 0, 1)$. Note that the units of the kinematic parameters are in radians and meters.

Table 7. Specification of the task.

Workpiece material	Mild steel
Joint torque limitation	49 Nm
Joint range limitation:	
Passive joints	$0 \sim 2\pi$
Active joints	$-\pi \sim \pi$

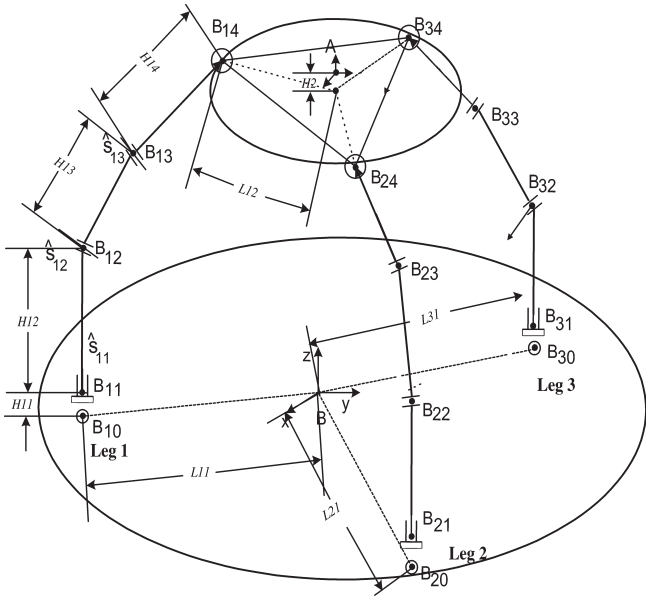

Figure 16. Geometric parameters of the RRRS-type three-legged parallel manipulator.

The simulation is coded in Matlab and carried out on a Pentium PII, 450 MHz personal computer. The time taken for the optimization is roughly 2 hours. To test the robustness of the algorithm, several initial configuration data-sets are taken. Figure 17 shows the convergence of the objective function of the parallel manipulator for three initial configuration data-sets. In each case, the optimal value of the objective function reached is 0.4563. For a comparison, it can be cited that the inverse of the condition numbers of the Stewart–Gough platform, modified Hexa, and SNU (Seoul National University) mechanism as studied in Kim *et al.* (2000) are 0.20533, 0.75757 and 0.00707 at home positions, respectively. Also the global conditioning indices of planar and spherical 3-DOF mechanisms, as studied in Gosselin and Guillot (1991), are reported to be 0.42961 and 0.52, respectively, and that of spherical 3-DOF mechanisms studied in Liu *et al.* (2000) is 0.58. The lengths of the optimized links for the specific task for first initial configuration data-set are $L_{11} = 0.6683$, $H_{12} = 0.1297$, $H_{13} = 0.1854$, $H_{14} = 0.4125$, and $L_{12} = 0.8$ (all dimensions are in meters). The lengths of the optimized links for the second and third initial configuration data-sets are (0.6712, 0.1253, 0.1712, 0.4342, 0.8) and (0.6734, 0.1282, 0.1741, 0.4093, 0.8) respectively. In each of the above three cases, the (1,3)-actuation scheme (first and third joints are actuated) is found to be better than the (1,2)-actuation scheme. This also depends upon the global representation of the task points, i.e. if the task points are away from the base frame, the (1,3)-actuation scheme is preferred. It is observed that all the performance measures give better values at the task point-1.

This optimal parallel manipulator is visualized in a visualization software called SEMORS-PKM. Figure 18 shows the parallel manipulator in a SEMORS-PKM application. Note that this parallel manipulator has first and third joints actuated which is the case for the (1,3)-actuation scheme.

6. Conclusion

Reconfigurable architecture is an important aspect of next-generation manufacturing. The addition of this feature to a parallel manipulator system calls for new methodologies for its application. In this paper, a two-stage methodology to determine the optimal configuration of reconfigurable parallel manipulators for specific tasks is discussed. This methodology is presented with specific reference to six-DOF three-legged parallel manipulators. With the aid of fixed- and variable-dimension modules, and the chosen functional requirements, a reconfigurable, robot assembly database is created. Then a `TaskToRobot` map is presented to map a task to possible types of parallel manipulators. Although this map is not exhaustive, it

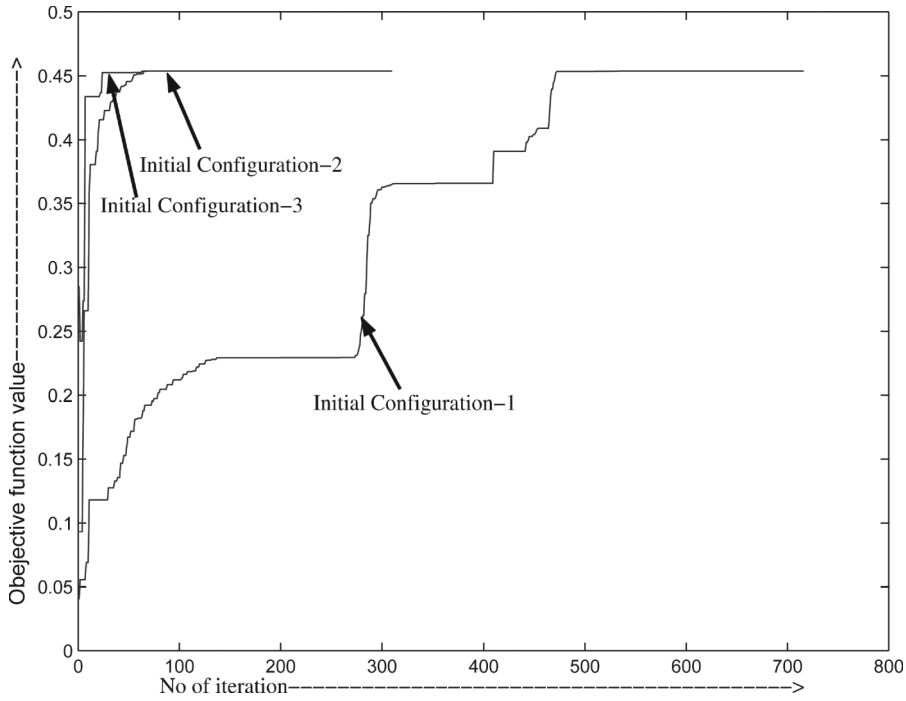

Figure 17. Convergence of the objective function.

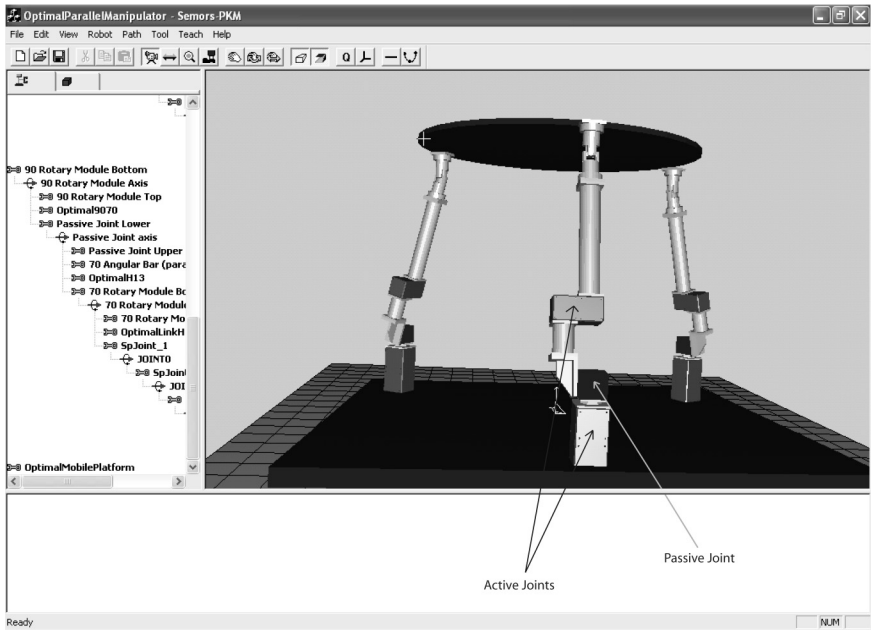

Figure 18. Optimal reconfigurable parallel manipulator in SEMORS-PKM application.

provides the user with ideas about the type of parallel manipulators to be chosen. In this mapping, the DOF of the task serves as the common criterion between task specified and the manipulator selected. Then design variables are identified which include the geometric lengths of different links. The actuation scheme is also identified as one of the design variables. It is shown that the actuation scheme significantly affects the performance of the manipulator. The product of the reciprocals of the condition number at different task points is chosen as the objective function. Reachability and joint torque limitations are formulated as constraints of the design optimization

problem. As the design space of the optimization problem includes both continuous (link dimensions) and discrete variables (actuation scheme), the Simplex method is used for this optimization problem. The design methodology is tested for a light machining task on a mild-steel workpiece. The algorithm converges to the same optimum value for different initial-configuration data-sets, which demonstrates its robustness. It is also observed and verified that the global coordinates of the task points affect the selection of the actuation scheme, i.e. with the changed position of the task points a different actuation scheme would have been preferred.

Acknowledgement

This work is supported by the Ministry of Education (Singapore) under the Academic Research Fund RG 29/99.

References

Ambrose, R.O., Design, construction and demonstration of modular, reconfigurable robots. PhD dissertation, University of Texas at Austin, 1991.

Angeles, J., *Fundamentals of Robotic Mechanical Systems: Theory, Methods and Algorithms*, 1997 (Springer Verlag: USA).

Bunday, B.D., and Garside, G.R., *Optimisation methods in Pascal*, 1987 (Edward Arnold Ltd: Australia).

Chen, I.M., Theory and applications of modular reconfigurable robotic systems, PhD dissertation, California Institute of Technology, 1994.

Chen, I.M. and Gao, Y., Closed-form inverse kinematics solver for reconfigurable robots. In *Proceedings of IEEE Conference on Robotics and Automation*, 2001, pp. 2395–2400, Seoul, Korea.

Cohen, R., Lipton, M.G., Dai, M.Q. and Benhabib, B., Conceptual design of a modular robot. *ASME Journal of Mechanical Design*, 1992, **114,** 117–125.

Dasgupta, B. and Mruthyunjaya, T.S., The stewart platform manipulator: a review. *Mech. Mach. Theory*, 2000, **35**(1), 15–40.

Dash, A.K., Chen, I.-M., Yeo, S.H. and Yang, G., Instantaneous kinematics and singularity analysis of three-legged parallel manipulators. In *Proceedings of IEEE/RSJ International Conference on Intelligent Robots and Systems*, 2001, pp. 1275–1280, Maui, USA. *Manufacturing science*. (John Wiley: USA).

Ghosh, A. and Mallik, A.K., *Manufacturing Science*, 1986 (John Wiley: USA).

Gosselin, C. and Guillot, M., A global performance index for the kinematic optimization of robotic manipulators. *ASME Journal of Mechanical Design*, 1991, **113,** 451–455.

Kim, J., Park, C., Kim, J. and Park, F.C., Performance analysis of parallel manipulator architectures for CNC machining. *Journal of Manufacturing Science and Engineering*, 2000, **122**(4), 753–759.

Kim, J.O. and Khosla, P., Design of space shuttle tile servicing robot: an application of task based kinematic design. In *Proceedings of IEEE Conference on Robotics and Automation*, 1993, pp. 867–874, Atlanta, GA.

Kim, S.G. and Ryu, J., Optimal design of 6 DOF parallel manipulators using three point coordinates. In *IEEE/RSJ International Conference on Intelligent Robots and Systems*, 2001, pp. 2178–2183, Maui, Hawaii.

Liu, X.-J., Jin, Z.-H. and Gao, F., Optimum design of 3-DOF spherical parallel manipulators with respect to the conditioning and stiffness indices. *Mech. Mach. Theory*, 2000, **35,** 1257–1267.

Merlet, J.P., Democrat: a design methodology for the conception of robots with parallel architecture. *Robotica*, 1997, **15,** 367–373.

Merlet, J.P., *Parallel Robots*, 2000 (Kluwer Academic: USA).

Paredis, C.J.J., An agent-based approach to the design of rapidly deployable fault tolerant manipulators, PhD dissertation, Carnegie Mellon University, 1996.

Park, F.C., Optimal robot design and differential geometry. *ASME Special 50th Anniversary Design Issue*, 1995, **117,** 87–91.

Podhorodeski, R.P. and Pittens, K.H., A class of parallel manipulators based on kinematically simple branches. *ASME Journal of Mechanical Design*, 1994, **116,** 908–914.

Ryu, J. and Cha, J., Optimal design of parallel manipulators for best accuracy. In *IEEE/RSJ International Conference on Intelligent Robots and Systems*, 2001, pp. 1281–1286, Maui, Hawaii.

Stamper, R.E., Tsai, L.W. and Walsh, G.C., Optimization of a three DOF translational platform for well-conditioned workspace. Technical Report TR97-71, Institute for Systems Research, University of Maryland, 1997.

Tsai, L.W., *Mechanism Design: Enumeration of Kinematic Structures According to Function*, 2000 (CRC Press: USA).

Ullman, D., *The mechanical design process*, 1992 (McGraw-Hill: New York).

Yang, G., Chen, I.M., Lim, W.K. and Yeo, S.H., Kinematic design of modular reconfigurable in-parallel robots. *Autonomous Robots*, 2001, **10**(1), 83–89.

Yang, G., Kinematics, dynamics, calibration, and configuration optimization of modular reconfigurable robots, PhD dissertation, School of Mechanical and Production Engineering, Nanyang Technological University, Singapore, 1999.